



Scholars Research Library

Der Pharma Chemica, 2015, 7(10):442-452
(<http://derpharmachemica.com/archive.html>)



ISSN 0975-413X
CODEN (USA): PCHHAX

Green synthesis of silver nanoparticles using lactose sugar and evaluation of their antimicrobial activity

Tayyebeh Madrakian¹, Sakineh Alizadeh^{1*}, Roya Karamian², Mostafa Asadbegyan²,
Morteza Bahram³ and Mohammad Javad Soleimani⁴

¹Faculty of Chemistry, Bu-Ali Sina University, Hamedan, Iran

²Department of Biology, Bu-Ali Sina University, Hamedan, Iran

³Department of Chemistry, Urmia University, Urmia, Iran

⁴Department of Plant Protection, Bu-Ali Sina University, Hamedan, Iran

ABSTRACT

In nanotechnology science several methods of chemical synthesis of silver nanoparticles (AgNps) are known. These methods involve high pressure, temperature and energy. Development in the green synthesis of Ag Nps is an important step in the field of application in nanotechnology. Accordingly, researchers are developing green methods that are eco-friendly, cost-effective and energy-efficient. Herein we report a green approach for the synthesis of AgNps. The colloidal silver particles were synthesized by reduction of AgNO₃ with D (+) lactose as a reducing agent. The morphology and structure of synthesized Ag Nps were characterized using Rayleigh scattering, transmission electron microscopy (TEM), UV/Vis spectrophotometry, dynamic light scattering (DLS) and X-ray diffraction method (XRD). Also the Ag Nps in different concentration and shapes were analyzed for their antimicrobial activity against 4 positive and negative bacteria using agar disc diffusion method and fungus *Fusarium oxysporum* cultivated on Potatoes Dextrose Agar medium (PDA). Results indicated that synthesized Ag Nps are relatively same in size (15 to 40 nm) and almost spherical. Also results showed that the AgNps had inhibition activity against tested microbials, especially on *Staphylococcus aureus* (+), (C₂₇: 16 ± 0.55 mm) and *Fusarium oxysporum* (0 to 100%). The effects of concentration and size of the synthesized Ag NPs on antimicrobial activity were also discussed.

Keywords: Silver nanoparticles, Green synthesis, Antibacterial activity, Antifungal activity, Central Composite Design.

INTRODUCTION

The application of nanoscale materials and structure (1 to 100 nm), is an emerging area of nanotechnology. The "green" chemistry approach to synthesizing biocompatible nanoparticles has gained attention in recent years. Plant extracts and other natural resources have been found to be an excellent alternative method for green synthesis of nanoparticles, since this method does not use any toxic chemicals and also has numerous benefits, including environmental friendliness, cost-effectiveness, and suitability for pharmaceutical and biomedical applications [1,2].

Metallic nanoparticles are one important group of materials that show great diversity and different uses. Among metallic nanoparticles, Ag NPs have been focused because they play a significant role in living organisms, biomedical [3], drug delivery [4], food industries [5], agriculture [6], textile industries [7], water treatment [8] as an antioxidant [9], antimicrobial [10], anti-cancer [11], cosmetics [12], ointments [13], and larvicides [14, 15]. Silver is well known as an effective antimicrobial material for treating wounds and chronic diseases [16]. It exhibits strong growth inhibition activity against a broad range of microorganisms.

The silver salts and silver metals have low antimicrobial activity and limited biomedical applications because they release silver ion too rapidly or too inefficiently [17]. Therefore, Ag NPs that possess high specific surface area and unique physicochemical properties have attracted abundance of interest in various fields, especially for production of antimicrobial agents [16-21]. A good green synthesis method can be useful for synthesis of well growth in size and efficiency of AgNPs, because size and yield of Ag nanoparticles play very important roles in inhibition of growing microorganism such as fungi and bacteria. The synthesis of AgNPs by tannic acid [22], gelatin and glucose [23], PVP and glucose [24] was already investigated.

In this study colloidal silver particles were synthesized by reduction of AgNO_3 with D (+) lactose as a reducing agent. The morphology and structure of synthesized Ag NPs were characterized using Rayleigh scattering, transmission electron microscopy (TEM), UV/Vis spectrophotometry, dynamic light scattering (DLS) and X-ray diffraction method (XRD). Central composite design (CCD) and response surface method (RSM) were applied to design the experiments and optimize the experimental parameters such as, concentration of silver nitrate, D (+) lactose, temperature, pH. In each experiment, concentration and size of nanoparticles were determined and collected as responses to construct the optimization model. Also under the optimum conditions, the inhibitory properties of Ag NPs against commercially important plant-pathogenic fungus (*Fusarium oxysporum*) and bacteria were studied.

MATERIALS AND METHODS

Chemicals and Solutions

All of the chemicals used in this work were purchased from Merck (Germany). Mueller-Hinton agar, Mueller-Hinton broth, nutrient broth and PDA mediums were purchased from Oxoid Ltd (Basingstoke, UK) and Sigma-Aldrich for the antimicrobial assays.

Synthesis of AgNPs

The protocol designed for the synthesis of AgNPs is simple. Aqueous AgNO_3 solution (1 mM) was prepared and used for the synthesis of Ag NPs. Colloidal silver particles were synthesized by reduction of AgNO_3 salt with D (+) lactose as a reducing agent. The initial concentrations of the reaction components were 1.0×10^{-1} mol L^{-1} for AgNO_3 , and 1.5×10^{-1} mol L^{-1} for the reducing agent. In the prepared solutions, the concentration of 1 mM AgNO_3 salt solution was varied in the range of 1.0×10^{-4} to 1.0×10^{-1} mol L^{-1} and the concentration of reducing agent (lactose) was varied from 1.5×10^{-3} to mol L^{-1} to 4.5×10^{-1} in NH_3 solution. The synthesis was done in water bath for 1.0 hour at optimum temperature.

Analysis of Silver Nanoparticles

The aliquot of reaction mixture was analysed by UV-vis spectrophotometer (Perkin-Elmer (Lambda2) spectrophotometer with a 1cm quartz cells) in the range of 400–700 nm. The size and morphology of the synthesized nanospheres were characterized by transmission electron microscopy (TEM, Philips-CMC-300 KV), on conventional carbon-coated copper grids. The size distribution of the AgNPs was calculated from the TEM images and the composition and crystal structure of the synthesized nanoparticles were determined by an X-ray diffractometer (XRD, 38066 Riva, d/G. via M. Misone, 11/D (TN) Italy) at ambient (25°C) temperature. Scattering spectra were obtained by Perkin Elmer (LS50B) luminescence spectrometer. The DLS experiments were conducted with a HORIBA L-550 at a fixed scattering angle of 90° and at a constant temperature of 25°C . A Metrohm model 713 pH-meter was used for pH measurements. A 40 kHz universal ultrasonic cleaner water bath (RoHS, Korea) was used.

Evaluation of Antibacterial Activity of AgNPs

Antibacterial activity of synthesized AgNPs were assessed against a panel of bacteria including two Gram positive bacteria, namely *Bacillus thuringiensis* (PTCC 1385) and *Staphylococcus aureus* (Wild), and two Gram negative bacteria, namely *Escherichia coli* (Wild) and *Serratia marcescens* (PTCC 1111) by disc diffusion method [25]. The AgNPs were dissolved in universal buffer solution to a final concentration of 1 mg mL^{-1} and then sterilized by filtration using 0.45 μm Millipore. All tests were carried out using 10 mL of suspension containing 1.5×10^8 bacteria mL^{-1} and spread on nutrient agar medium. Negative controls were prepared by using universal buffer solution. Gentamicin, penicillin and cephalixin were used as positive reference standards.

Evaluation of Antifungal Activity of AgNPs

Antifungal activity of AgNPs was assessed against *Fusarium oxysporum*. *Fusarium oxysporum* was cultivated in Potatoes Dextrose Agar (PDA) medium. AgNPs in different concentrations were added to cultivation medium. In order to make the control group, double distilled water was added only to one of the

plates. After a 7-day incubation of fungus on culture medium containing AgNPs, radial growth of fungal mycelium was recorded. Diameter and the number of colonies in treated groups were compared with those of controls. The sampling was repeated 24 times. The following formula "Eq.(A₁)" was used for calculation of the inhibition rate (%):

$$\text{Inhibition rate (\%)} = (R-r/R) \times 100$$

Where, R is the radial growth of fungal mycelia on the control plate and r is the radial growth of fungal mycelia on the plate treated with AgNPs.

Statistical Analysis

All calculations and programming for Ag Npsynthesis were performed in MATLAB (Hyper-cube Inc. Version10) software. The essential regression and experimental design for chemists and engineers (EREGRESS) excel add in software. Multiple linear regression (MLR) was used in modeling the relationship between two or more interpretive variables and a response variable obtained by fitting a linear equation. The mean values in DLS spectra and peak area of scattering spectra were used as response vectors for size and yield controlled synthesis. In this research effect of different parameters such as saccharide concentration (Csach), pH, temperature (temp) and AgNO₃ concentration (CAgNO₃) on Ag NPs synthesis was investigated. Central composite experimental design (CCD) was applied in simultaneous optimization of these parameters. The designed 28 experiments were shown in Table 1. Peak area of scattering spectra and mean value of DLS spectra were obtained as analytical responses.

Table 1: Parameters used for AgNPs synthesis, size and peak area of scattering spectra for each synthesis

Exp #	pH	Ag* (g)	La** (g)	temp*** (°c)	Size(nm)	Peak area
1	9.5	0.0505	0.505	75	59	855.4
2	8.25	0.02575	0.7525	67.5	118	855.4
3	8.25	0.02575	0.2575	82.5	60	432.32
4(cp)****	9.5	0.0505	0.505	75	50	723.18
5	12	0.0505	0.505	75	4	2055
6	8.25	0.07525	0.7525	82.5	100	920.78
7	10.75	0.07525	0.2575	82.5	200	12249
8	8.25	0.07525	0.2575	82.5	250	673.27
9	7	0.0505	0.505	75	40	283.29
10	8.25	0.07525	0.7525	67.5	240	9270
11	8.25	0.07525	0.2575	67.5	3	746.24
12(cp)	9.5	0.0505	0.505	75	99	4470
13	10.75	0.07525	0.7525	67.5	200	4470
14(cp)	9.5	0.0505	0.505	75	250	686.04
15	9.5	0.1	0.505	75	65	243.35
16	9.5	0.001	0.505	75	300	1353
17	10.75	0.02575	0.7525	67.5	61	4689
18	9.5	0.0505	1	75	25	1353
19	9.5	0.0505	0.505	90	21	938.54
20	10.75	0.02575	0.2575	82.5	300	3666
21	10.75	0.07525	0.2575	67.5	250	443.75
22	10.75	0.02575	0.7525	82.5	40	5454
23	10.75	0.02575	0.2575	67.5	24	150.6
24	9.5	0.0505	0.01	75	80	5960
25	9.5	0.0505	0.505	60	70	5331
26	10.75	0.07525	0.7525	82.5	100	579.3
27	8.25	0.02575	0.7525	82.5	150	5161
28	8.25	0.02575	0.2575	67.5	25	579.3

*Ag: (AgNO₃ solution)

**La: (Lactose) in gram

***Temp: (Temperature)

**** Central point

Data obtained from antimicrobial assays are the average of triplicate analyses and recorded as means ± standard deviation. Statistical analysis was performed using Student's t-test, and *p* value < 0.05 was regarded as significant.

RESULTS AND DISCUSSION

Formation of the Ag NPs

The formation of Ag NPs was observed upon the colourchange of the mixture from transparent yellow into brown, as shown in Figure 1, due to the coherentoscillation of electrons at the surface of NPs, resulting in surface plasmon resonance (SPR) [26]. The observed colour change primarily in the reaction mixture was

within 10 min that indicated the formation of AgNPs in the solution. The colour intensity increased significantly with increasing the AgNO_3 concentration at a fixed volume of D (+) lactose (as a reducing agent). This change of colour and intensity of the SPR band might be due to the variation in concentration, size, and shape of the resulting Ag NPs [27]. The UV-vis spectrophotometry was also used to confirm the formation of the Ag NPs as shown in Figure 3B.



Fig.1: The colour change of the mixture from transparent yellow into brown after 24 hours of reaction

Size and Structure of the Silver Nanoparticles

The morphology and size distribution of the synthesized AgNPs were determined by TEM analysis. The TEM image in Figure 2A shows that the particles were almost spherical. The histogram of particle size distribution for the AgNPs (Figure 2B) suggest that the particles are relatively same in size and ranged in size from 15 nm to 40 nm with an average diameter of 23 nm. At lower the concentrations of lactose, more silver atoms will aggregate into a nanoparticle, which results in increased diameters. Particle sizes were measured according to the statistical analysis of large number (20–50) of particles.

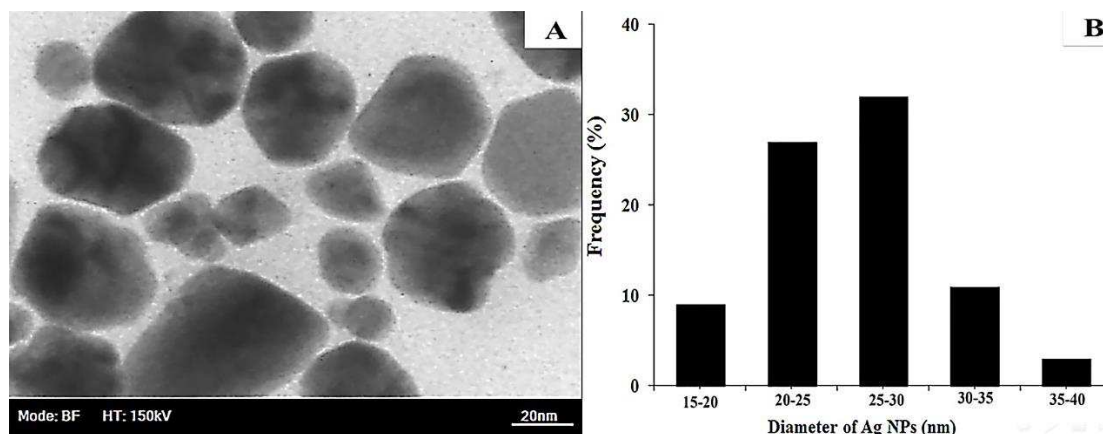


Fig. 2: A: Transmission electron microscopic image of Ag NPs obtained using D (+) lactose after 24 hours of reaction B: The particle size distribution

The synthesized AgNPs were further characterized using X-ray diffractometry. The X-ray diffraction pattern showed four intense peaks (36.5° , 43.8° , 64.7° , 78.1°) in the whole spectrum of 2θ values ranging from 10° to 90° , which correspond to the (111), (200), (220), and (311) crystallographic planes of face-centered spherical silver, respectively (Figure 3A).

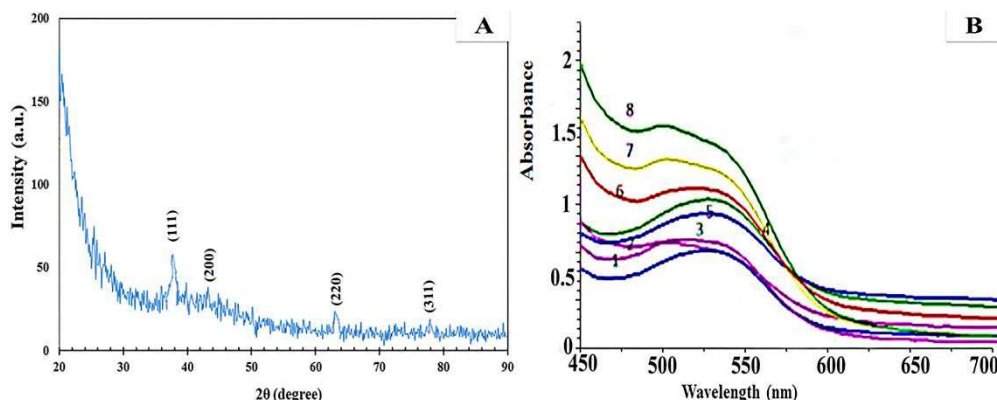


Fig. 3: A: X-ray diffraction patterns of the prepared Ag NPs with modified Tollen's method (pH 9.5, AgNO₃ 0.050 g, Lactose 0.5 g, temperature 75 °C). B: Ultraviolet-visible absorption spectrum of Ag NPs synthesized using D (+) lactose according to Table 1 (conditions the same as experiment 1)

Evaluation of Method Performance in Yield and Size Controlled Synthesis

As mentioned, in order to study the effect of synthesis parameters and their possible central composite experimental design was used (Table 2). The studied chemical parameters were concentration of silver nitrate (AgNO₃), concentration of D (+)-lactose, temperature and pH which were varied in 5 levels. Because the P-value for each parameter is greater than 0.05, therefore it has no significant effect in the model (the confidence interval of 95%), and can be removed (the value of parameter coefficient is taken zero). But the model was kept hierarchical, i.e. a factor that has the P-value greater than 0.05 but the higher order of this factor has the P-value less than 0.05 was not removed but if square (second order) parameters to be important with acceptable P-value; we must use first order of these parameters in another model. In this model, EREGRESS software was used i.e. another model was made for interpreting the effect of both first and second order and other forms of parameters. In case good fitting was not done with conventional model and R^2 , R^2_{adj} and R^2_{pred} in conventional model were not good, the logarithmic form was used; this way also eliminated the effect of the units. According to Table 2a the important parameters are $\log C_{AgNO_3} \times \log T$, $\log C_{AgNO_3}$, $pH \times \log C_{Lac}$, $(\log C_{AgNO_3})^2$, pH , $\log C_{Lac}$, $\log T$, $\log T \times \log C_{Lac}$. According to these important parameters equation of yield controlled synthesis was developed which is shown below.

$$Y = -0.37 - 0.84(\log C_{AgNO_3} \times \log T) - 0.7 \log C_{AgNO_3} + 0.45 (pH \times \log C_{Lac}) + 0.075(\log C_{AgNO_3})^2 + 2.5(pH) - 2.4 (\log C_{Lac}) + 1.8 (\log T) - 0.73 (\log T \times \log C_{Lac})$$

The greater coefficient shows the more effective parameter. According to the following equation, the most important parameter in increasing the yield is pH and its effect is positive on the yield i.e. by increasing the pH, the yield of nanoparticles increase. Other parameters, including $\log C_{Lac}$, $\log T$, $\log C_{AgNO_3} \times \log T$, $\log T \times \log C_{Lac}$, $\log C_{AgNO_3}$, $pH \times \log C_{Lac}$, $(\log C_{AgNO_3})^2$ are also important. $pH \times \log C_{Lac}$, $(\log C_{AgNO_3})^2$, pH and $\log T$ have positive sign i.e. have effect in increasing the yield, but $\log C_{AgNO_3} \times \log T$, $\log C_{Lac}$, $\log T \times \log C_{Lac}$ and $\log C_{AgNO_3}$ have negative sign i.e. they decrease the yield. The least important coefficient is $(\log C_{AgNO_3})^2$. The positive sign of coefficient describes that with its increasing, the response is also increased. Interaction parameters are $pH \times \log C_{Lac}$, $\log T \times \log C_{Lac}$ and $\log C_{AgNO_3} \times \log T$ which show that combination of temperature and concentration of silver nitrate and pH have important effect among other interaction parameters. The model showed that other parameters have no significant effect on the yield of silver nanoparticles formation. A key aim of experiment was to determine how significant a factor was. It is discussed how to design an experiment so that allows sufficient degrees of freedom to determine the significance of a given factor. In the following section, the procedure of proving the significance of a factor is discussed. There are many situations in which this information is useful. After checking the different parameters in CCD, one model is made for obtaining the best conditions of synthesis which get the response as a function of effective parameters. MLR is used for modelling and the coefficients are calculated (Table 2b). As mentioned before response matrices were mean values of DLS spectra for size controlled synthesis. Data matrices were different combinations of parameters. As demonstrated in previous model the greater coefficient shows the more effective parameter and the positive signs of the coefficient describe that with its increasing, the response is increased as well. According to the following equation the most important parameter in increasing the size is $\log C_{Lac}$. Other parameters, including $\log T$, pH , $(\log T)^2$, $(\log C_{Lac})^2$, $\log C_{AgNO_3}$ and $\log C_{Lac} \times \log C_{AgNO_3}$ are also important. The least important coefficient in increasing the size is $\log C_{Lac} \times \log C_{AgNO_3}$. The only interaction parameter that showed no significant effect was $\log C_{Lac} \times \log C_{AgNO_3}$ which shows the interaction of concentration of lactose and AgNO₃ in the log form. According to these important parameters, equation of size controlled synthesis was developed which is shown below.

$$Y = 0.55 + 0.059(\log C_{lac} \times \log C_{AgNO_3}) - 0.5(\log T)^2 + 0.49(\log C_{lac})^2 + 0.79 \log T + 0.16 \log C_{AgNO_3} + 0.683 pH - 1.19 \log C_{lac}$$

Table 2: Experimental variables, levels, design table and results of the central composite design for (a) yield controlled (b) size controlled synthesis of AgNPs with modified Tollen's method

Parameter	Coefficient	Standard error	T for H ₀	P-value
(a) For yield controlled synthesis				
Intercept	-0.37	2.81	-0.13	0.9
LogC _{AgNO₃} × LogT	-0.84	0.44	-1.92	0.07
pH × LogC _{Lac}	0.45	0.29	1.53	0.14
(Log C _{AgNO₃}) ²	0.075	0.031	2.41	0.024
pH	2.5	1.15	2.16	0.041
logC _{AgNO₃}	-0.7	1.03	-1.5	0.023
LogC _{Lac}	-2.4	1.15	-2.12	0.044
Log T	1.8	0.34	2.19	0.033
Log T × LogC _{Lac}	-0.73	0.51	-1.8	0.05
(b) For size controlled synthesis				
Intercept	0.55	0.16	3.37	0.002
LogC _{Lac}	1.19	0.19	-6.09	0.0001
pH	0.68	0.19	3.64	0.001
LogT	0.79	0.07	10.99	0.0001
LogC _{Lac} × LogC _{AgNO₃}	0.059	0.02	2.30	0.028
(LogC _{Lac}) ²	0.49	0.21	2.39	0.023
LogC _{AgNO₃}	0.16	0.02	8.20	0.0001
(LogT) ²	-0.5	0.18	2.83	0.008

Response surface and selection of optimum conditions

For obtaining the optimum conditions of studied parameters, the response surface plots were used. The optimum values can be concluded using plots represented in Figure 4 and 5. In these plots all the minimum or maximum values of z (yield) in x (logC_{Lac}) or y (pH) direction were investigated. As mentioned above, in three figures difference of temperature was investigated, which showed that x and y axis had different behaviour across the z axis at minimum (67.5), medium (75) and maximum (90°C) values of temperature. These prove that temperature is one of the important parameters in yield controlled synthesis of silver nanoparticles. In different amounts of x (logC_{Lac}), some optimum points of z (yield) exist in one y (pH) value which proves that x and y interact. This occurs in different amounts of y (pH) in one x value. The response surface plot was also used for size controlled synthesis. The results are shown in

Figure 2 and 3. In these plots all minimum or maximum values of z (size) in x (logC_{Lac}) and y (logT) directions were investigated. As mentioned above, in three figures difference of AgNO₃ concentration were investigated, which showed that x and y axis had different behaviours along the z axis at minimum (0.001), medium (0.01) and maximum (0.1M) values of AgNO₃ concentration. These prove that AgNO₃ concentration is one of the important parameters in size controlled synthesis of silver nanoparticles. In different amounts of x (logC_{Lac}), some optimum points of z (size) exist in one y (pH) value which proves that x and y have interaction. This occurs in different amount of y (pH) in one x value.

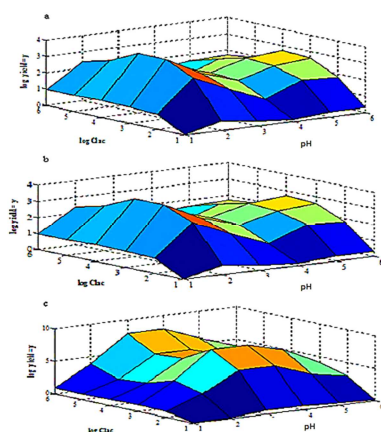


Fig.4: Response surface plot based on two factors (logC_{Lac} and pH) for yield controlled synthesis at three temperature levels ((a) 67.5, (b) 75, (c) 90) °C

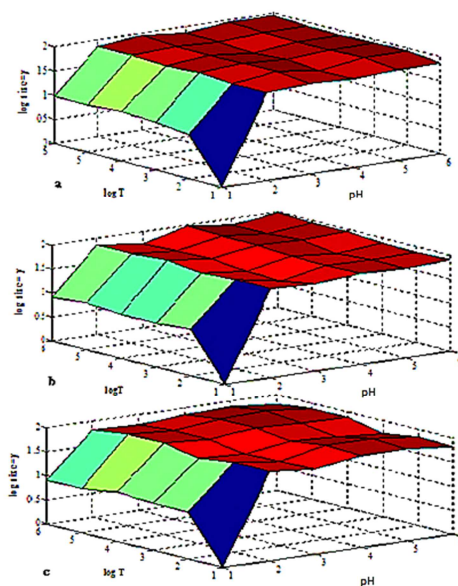


Fig.5: Response surface plot based on two factors (logT and pH) for size controlled synthesis at three AgNO₃ concentration levels (a) 0.001,(b) 0.01 and (c) 0.1M

Table 3: Evaluation of ANOVA parameters for (a) yield controlled (b) size controlled synthesis of AgNPs

Source	D.F	Sum of squares	Mean Squares	F value	P-value
(a) For yield controlled synthesis					
Total	27	660.92	16.94	4940.29	0.0001
Regression	7	659.10	94.15		
Error	20	0.61	0.02		
Lack of Fit	17	0.31	0.014	1.71	
Pure Error	3	0.30	0.033		
(b) For size controlled synthesis					
Total	27	492.01	12.62	649.65	0.0001
Regression	7	488.50	69.80		
Error	20	3.44	0.11		
Lack of fit	17	1.36	0.21	1.43	
Pure error	3	2.08	0.06		

Analysis of Variance of the model

An analysis of variance (ANOVA) of the constructed model is shown in Table 3a, The F-value of the model (regression) describes that the regression at the confidence interval of 95.0% ($P=0.05$) is significant and the variance due to regression is equal to the variance due to error in the experiment. The adjusted correlation coefficient (R_{adj}^2) of 0.98 explaining 98.0% of variance in the response value is related to the considered factors. The model has a root-mean square error (RMSE) of 0.14 and coefficient of variation of 2.10 that corresponds to 2.10% error in the synthesis. In the confidence interval of 95%, the model shows important parameters. The null hypothesis describes that the value of the parameter coefficient is zero. According to Table 2, all of parameters have P-value less than 0.05 that show all parameters are important and we cannot neglect any of them. The analysis of variance (ANOVA) of the model is shown in Table 3b. In Table 4 the parameters of model evaluation were collected; these show total, regression, error and lack of fit with degree of freedom, mean square, F-value and unique P value of the model. One model was selected as a well-defined model for good R^2 and R^2 prediction and tolerable standard error (Table 4b). The F-value of the model (regression) describes that the regression at the confidence interval of 95.0% ($P=0.05$) is significant and the variance due to regression is equal to the variance due to error in the experiment. The adjusted correlation coefficient (R_{adj}^2) of 0.97 explaining 97.0% of variance in the response value is related to the considered factors.

The model has a root-mean square error (RMSE) of 0.31 and coefficient of variation (C.V) of 5.37 that corresponds to 5.37% error in the synthesis. In the confidence interval of 95%, the model shows important parameters. In Figure 4 the calculated response (y) from the model is plotted vs. the measured (y) for (a) yield controlled and (b) size controlled synthesis. This shows that the model has a good predictive ability in the log form. The R^2 for this plot is the same as that calculated for the model (adjusted correlation coefficient = 0.98 and 0.97) for yield and size controlled synthesis, respectively. Also in Figure 5 residual plot shows closeness of the obtained response to the predicted response.

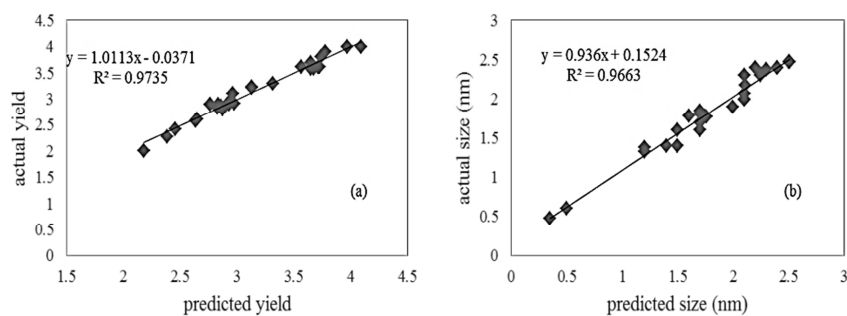


Fig. 6: Plot of the actual response from the model vs. the predicted response (plot of y vs. y^{\wedge}) for (a) yield controlled (b) size controlled synthesis

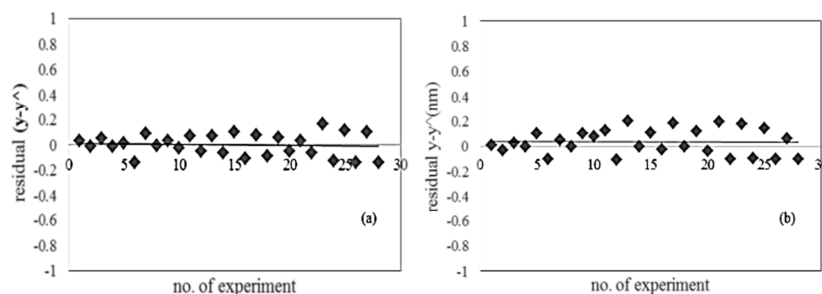


Fig.7: Plot of the residual vs. number of experiment for (a) yield controlled (b) size controlled synthesis

Table 4: Some statistic parameters for evaluation of modelin (a) yield controlled (b) sizecontrolled synthesis of silver nanoparticles. (R^2 , R_{adj}^2 , R^2_{pred} , RMSE, Dept. Mean and C.V)

R^2	R_{adj}^2	R^2_{pred}	RMSE	Mean	C.V.
(a) For yield controlled synthesis					
0.98	0.98	0.97	0.14	4.02	2.1
(b) For size controlled synthesis					
0.98	0.97	0.96	0.31	3.21	5.37

Antibacterial activity

The inhibition zone values were determined for the Ag NPs synthesized using lactose sugar against four types of Gram positive and negative bacteria. The results are presented in Table 5 and positive and negative controls in Table 6 and Figure 6. The tested AgNPs (In different concentrations and sizes) were dissolved in universal buffer. Since universal buffer was used as a solvent, it was also screened against all bacteria included in this study and no activity was found. The samples C_7 , C_{13} , C_{15} , C_{16} and C_{24-27} showed more antibacterial activity against bacterial species included in the study. However, most of the samples had the highest antibacterial activity against *Staphylococcus aureus* (+) but in contrast, *Bacillus thuringiensis* (+) was the most resistant bacterium (Table 5). It is well known that *Staphylococcus aureus* (+) and *Bacillus* species are food poisoning agents [28]. Among 28 AgNPs, only C_{28} showed antibacterial activity on all bacterial tested in this research. Generally antibacterial activity of compounds is attributed mainly to its major components. However, today it is known that the synergistic or antagonistic effect of one compound in minor percentage of mixture has to be considered [29-31]. The antibacterial activities of the AgNPs in all samples did not promote by increasing concentration of $AgNO_3$ and reduce size of AgNPs. This is reasonable due to synergistic or antagonistic effect of different parameters such as saccharide and $AgNO_3$ concentrations, AgNPs size and synthesis temperature. Also, it has been reported that the pathogenic effect of the NPs can be attributed to their stability in the medium as colloids, which modulates the phosphotyrosine pattern of the pathogen proteins and consequently arrests their growth. Moreover, it was proposed that the variation in the growth inhibition of bacteria by NPs may be attributed to the presence of peptidoglycan, which has a strong negative complex structure [32]. When comparing the antibacterial activity of the tested samples to those of reference antibiotics, the inhibitory potency of some tested compounds were found to be good. All bacteria tested were resistant to Penicillin, while the antibacterial effects of some samples were higher than those of Penicillin on these bacteria (Table 6 and Figure 6). Reports on the mechanism of inhibitory action of silver compounds on microorganisms show that upon Ag treatment, DNA loses its replication ability and expression of ribosomal subunit proteins as well as some other cellular proteins and enzymes essential to ATP production becomes inactivated [33]. The above results

indicating the potential of the prepared Ag NPs as antibacterial agents; however, further investigations are required to explore their bactericidal effects on other types of bacteria.

Table 5: Antibacterial activities of the synthesized AgNps

Samples	Conc. and size	Inhibition zone (mm)			
		<i>S. a</i> (+)	<i>B. t</i> (+)	<i>E. c</i> (-)	<i>S. m</i> (-)
C ₁	C: 2×10 ⁻⁵ S:59	7 ± 0.26 ^a	8 ± 0.16 ^a	Na	Na
C ₂	C:10 ⁻⁵ S:118	7 ± 0.33 ^a	7 ± 0.10 ^b	7 ± 0.24 ^a	7 ± 0.33 ^a
C ₃	C:10 ⁻⁵ S:60	7 ± 0.54 ^a	Na	7 ± 0.28 ^a	7 ± 0.54 ^a
C ₄	C: 2 ×10 ⁻⁵ S:50	7 ± 0.21 ^a	Na	Na	Na
C ₅	C: 2 ×10 ⁻⁵ S:4	Na	Na	Na	Na
C ₆	C: 3 × 10 ⁻⁴ S:100	Na	Na	Na	Na
C ₇	C: 2 ×10 ⁻⁵ S:200	11 ± 0.55 ^b	Na	7 ± 0.11 ^a	Na
C ₈	C: 3 × 10 ⁻⁴ S:250	8 ± 0.43 ^c	Na	7 ± 0.22 ^a	Na
C ₉	C: 4 × 10 ⁻⁵ S:40	7 ± 0.16 ^a	Na	9 ± 0.14 ^b	Na
C ₁₀	C:3 ×10 ⁻⁴ S:240	7 ± 0.14 ^a	Na	Na	Na
C ₁₁	C: 2 × 10 ⁻⁵ S:3	7 ± 0.22 ^a	Na	7 ± 0.16 ^a	Na
C ₁₂	C: 3 ×10 ⁻⁴ S:99	7 ± 0.35 ^a	Na	Na	Na
C ₁₃	C: 3 ×10 ⁻⁴ S:200	15 ± 0.33 ^d	Na	Na	Na
C ₁₄	C: 3 ×10 ⁻⁴ S:250	7 ± 0.16 ^a	Na	Na	7 ± 0.12 ^a
C ₁₅	C: 4 ×10 ⁻⁵ S:65	14 ± 0.64 ^d	Na	Na	Na
C ₁₆	C: 4 × 10 ⁻⁷ S:300	12 ± 0.54 ^b	Na	Na	Na
C ₁₇	C: 10 ⁻⁵ S:61	9 ± 0.26 ^f	Na	7 ± 0.25 ^a	7 ± 0.33 ^a
C ₁₈	C: 2×10 ⁻⁵ S:25	8 ± 0.33 ^c	Na	Na	Na
C ₁₉	C: 2 × 10 ⁻⁵ S:21	8 ± 0.00 ^c	Na	Na	Na
C ₂₀	C: 10 ⁻⁵ S:300	7 ± 0.22 ^a	Na	Na	Na
C ₂₁	C: 3 × 10 ⁻⁴ S:250	7 ± 0.27 ^a	Na	8 ± 0.43 ^c	7 ± 0.22 ^a
C ₂₂	C:10 ⁻⁵ S:40	Na	Na	Na	Na
C ₂₃	C:10 ⁻⁵ S:24	8 ± 0.11 ^a	Na	Na	7 ± 0.12 ^a
C ₂₄	C:2 × 10 ⁻⁵ S:80	11 ± 0.25 ^b	Na	Na	7 ± 0.28 ^a
C ₂₅	C: 2 × 10 ⁻⁵ S:70	10 ± 0.17 ^e	8 ± 0.15 ^a	Na	7 ± 0.15 ^a
C ₂₆	C: 3 × 10 ⁻⁴ S:100	13 ± 0.34 ^b	Na	Na	Na
C ₂₇	C: 10 ⁻⁵ S:150	16 ± 0.55 ^d	7 ± 0.22 ^b	Na	Na
C ₂₈	C: 10 ⁻⁵ S:25	10 ± 0.15 ^e	11 ± 0.17 ^c	7 ± 0.25 ^a	8 ± 0.10 ^b

Experiment was performed in triplicate and expressed as mean ± SD. Values with Different superscripts within each column (for any bacteria in different concentrations) are significantly different ($P < 0.05$).

Na: No active

Table 6: Antibacterial activities of 3 antibiotics as positive Controls and universal buffer solvent as negative control

Microorganism	Inhibition zone (mm)			
	Positive controls			Negative control
	Gentamicin	Penicillin	Cephalexin	Universal buffer
<i>S. a</i> (+)	30 ± 0.14	Na	15 ± 16	Na
<i>E. c</i> (-)	Na	Na	Na	Na
<i>B. t</i> (+)	25 ± 0.18	Na	22 ± 24	Na
<i>S. m</i> (-)	35 ± 0.24	Na	Na	Na

Experiment was performed in triplicate and expressed as mean ± SD.

Na: No active

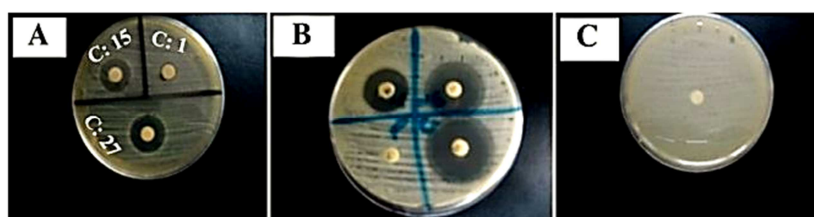


Fig. 6: Antibacterial activities of some samples against *Staphylococcus aureus* (+) A: Antibacterial activity of samples C₁, C₁₅ and C₂₇ B: Antibacterial activity of positive controls C: C: Antibacterial activity of negative control (universal buffer)

Antifungal activity

The inhibition zone values were determined for the AgNPs synthesized against *Fusarium oxysporum* fungus. The results are presented in Table 7 and Figure 7. *Fusarium oxysporum* are ubiquitous soil inhabitants that attacks its host by entering through the root and grows in the plant xylem, eventually blocking the vascular system. This prevents transport of water and nutrients to the rest of the host, causing wilting, discoloration, and can cause severe losses in a wide variety of crop and ultimately death of the plants of great economic importance [34, 35]. In agriculture, application of large amount of synthetic fungicides has been considered to be one of the cheapest and most common approaches to control plant diseases [36]. These fungicides usually are difficult

to degrade and are toxic to humans and animals. Phytopathogens also have developed resistance to frequent pesticides, leading to the decreasing of efficiency [37]. Therefore, the search for bioactive compounds from terrestrial and marine-derived endophytic fungi which are safe and more environmentally friendly were introduced to replace the synthetic fungicides. Results from antifungal assessments of the samples are presented in Table 7. It was determined that the solvent (universal buffer) as negative control had no antifungal activity against *Fusarium oxysporum* (Table 7 and Figure 7). All samples showed good antifungal activities. Among 28 AgNps, only C₈ samples exhibited weak antifungal activity against *Fusarium oxysporum*. Antifungal activities of the AgNps in all samples did not promote by increasing concentration and reduce size. This is reasonable because synergistic or antagonistic effect of different parameters such as saccharide, AgNO₃ concentrations, AgNps size and synthesis temperature. The above results indicate that the AgNps studied in this research may be used in treatment of plant diseases caused by *Fusarium oxysporum* and also increase in a wide variety of crop of the plants.

Table 7. Antifungal activities of the synthesized AgNps

Compounds	Inhibition radial growth of fungal mycelium (%)	
	Conc.and size(nm)*	<i>F. oxysporum</i>
C ₁	C: 2×10 ⁻⁵ S:59	100
C ₂	C:10 ⁻⁵ S:118	100
C ₃	C:10 ⁻⁵ S:60	Na
C ₄	C: 2 ×10 ⁻⁵ S:50	100
C ₅	C: 2 ×10 ⁻⁵ S:4	100
C ₆	C: 3 × 10 ⁻⁴ S:100	100
C ₇	C:2 ×10 ⁻⁵ S:200	100
C ₈	C: 3 × 10 ⁻⁴ S:250	100
C ₉	C: 4 × 10 ⁻⁵ S:40	35.01
C ₁₀	C: 3 ×10 ⁻⁴ S:240	100
C ₁₁	C: 2× 10 ⁻⁵ S:3	100
C ₁₂	C: 3 ×10 ⁻⁴ S:99	100
C ₁₃	C: 3 ×10 ⁻⁴ S:200	100
C ₁₄	C: 3 ×10 ⁻⁴ S:250	100
C ₁₅	C: 4 ×10 ⁻⁵ S:65	Na
C ₁₆	C: 4 ×10 ⁻⁷ S:300	100
C ₁₇	C: 10 ⁻⁵ S:61	100
C ₁₈	C: 2 ×10 ⁻⁵ S:25	100
C ₁₉	C: 2 × 10 ⁻⁵ S:21	Na
C ₂₀	C: 10 ⁻⁵ S:300	48.6
C ₂₁	C: 3 × 10 ⁻⁴ S:250	Na
C ₂₂	C: 10 ⁻⁵ S:40	100
C ₂₃	C: 10 ⁻⁵ S:24	100
C ₂₄	C: 2 × 10 ⁻⁵ S:80	35.01
C ₂₅	C: 2 × 10 ⁻⁵ S:70	100
C ₂₆	C: 3 × 10 ⁻⁴ S:100	35.99
C ₂₇	C: 10 ⁻⁵ S:150	100
C ₂₈	C: 10 ⁻⁵ S:25	100

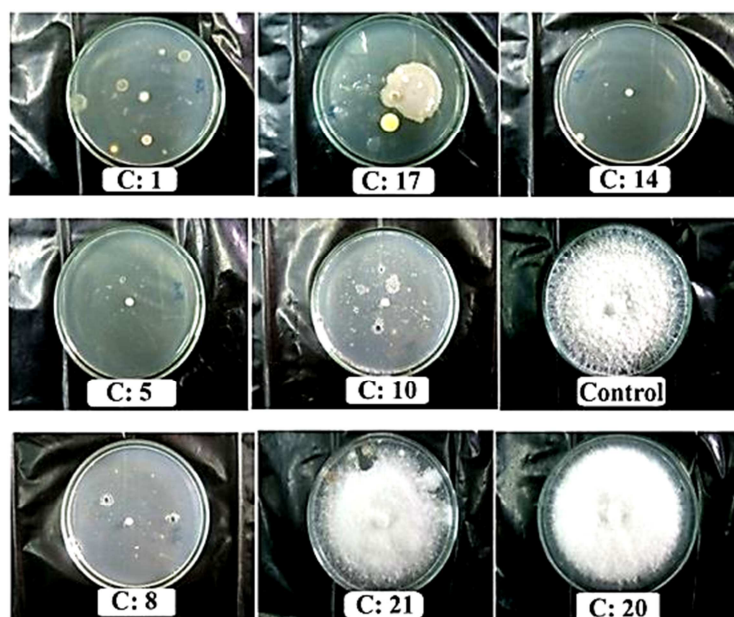


Fig. 7: Antifungal activities of the synthesized silver nanoparticles (label is the number of synthesis in Table 10) and control

CONCLUSION

We have demonstrated a good method for developing a simple, safe, cost-effective, and ecofriendly preparation of AgNPs by D (+) lactose as a reducing agent. The synthesized AgNPs had an average particle size of 23 nm and a spherical structure. Results obtained from present study clearly demonstrated that the Ag NPs exhibit acceptable antibacterial and antifungal activities, which might be helpful in preventing the progress of various infections and can be used as alternative systems for medicines and agricultural. Future research should envision studies on modification of these compounds to increase their biological activities. The results were proved that which parameters changed yield and size of synthesis that affect the antifungal and antibacterial effect of plants pathogens.

Acknowledgements

This work was supported by the Bu-Ali Sina University Research Council and Center of Excellence in Development of Environmentally Friendly Methods for Chemical Synthesis (CEDEFMCS) and the authors are grateful for their kind support.

REFERENCES

- [1] J.A. Dahl, B.L.S. Maddux, J.E. Hutchison, *Chem. Rev.*, **2007**, 107, 2228.
- [2] J.E. Hutchison, *ACS Nano.*, **2008**, 2, 395.
- [3] K. Chaloupka, Y. Malam, A.M. Seifalian, *Trends Biotech.*, **2010**, 28, 580–588.
- [4] T.W. Prow, J.E. Grice, L.L. Lin, R. Faye, M. Butler, W. Becker, E.M.T. Wurm, C. Yoong, T.A. Robertson, H.P. Soyer, M.S. Roberts, *Adv. Drug Deliv. Rev.*, **2011**, 63, 470–491.
- [5] Q. Chaudhry, L. Castle, *Trends Food Sci. Tech.*, **2011**, 22, 595–603.
- [6] R. Nair, S.H. Varghese, B.G. Nair, T. Maekawa, Y. Yoshida, D. Sakthi Kumar, *Plant Sci.*, **2010**, 179, 154–163.
- [7] F.M. Kelly, J.H. Johnston, *ACS Appl. Mater. Interfaces.*, **2011**, 3, 1083–1092.
- [8] T.A. Dankovich, D.G. Gray, *Environ. Sci. Technol.*, **2011**, 45, 1992–1998.
- [9] K.L. Niraimathi, V. Sudha, R. Lavanya, P. Brindha, *Colloid. Surface B.*, **2013**, 102, 288–29.
- [10] R. Sankar, A. Karthik, A. Prabu, S. Karthik, K.S. Shivashangari, V. Ravikumar, *Colloid. Surface B.*, **2013**, 108, 80–84.
- [11] S.C. Boca, M. Potara, A.M. Gabudean, A. Juhem, P.L. Baldeck, S. Astilean, *Cancer Lett.*, **2011**, 31, 131–140.
- [12] J. Jain, S. Arora, J.M. Rajwade, P. Omray, S. Khandelwal, K.M. Paknikar, *Mol. Pharm.*, **2009**, 6, 1388–1401.
- [13] C.J. Murphy, *J. Mater. Chem.*, **2008**, 18, 2173–2176.
- [14] S.M. Roopan, Rohit, G. Madhumitha, A. Abdul Rahuman, C. Kamaraj, A. Bharathi, T.V. Surendra, *Ind. Crop Prod.*, **2013**, 43, 631–635.
- [15] U. Jagtap, V.A. Bapa, *Ind. Crop Prod.*, **2013**, 46, 132–137.
- [16] M. Rai, A. Yadav, A. Gade, *Adv. Biotech.*, **2009**, 27, 76–83.
- [17] J.S. Kim, E. Kuk, K.N. Yu, J.H. Kim, S.J. Park, H.J. Lee, S.H. Kim, Y.K. Park, Y.H. Park, C.Y. Hwang, Y.K. Kim, Y.S. Lee, D.H. Jeong, M.H. Cho, *Nano. Nanotech. Biol. Med.*, **2007**, 3, 95–101.
- [18] J. Soukupova, L. Kvitek, A. Panacek, T. Nevecna, R. Zboril, *Mater. Chem. Phys.*, **2008**, 111, 77–81.
- [19] Y.A. Krutyakov, A.A. Kudrinskiy, A.Y. Olenin, G.V. Lisichkin, *Russ. Chem. Rev.*, **2008**, 77, 233–235.
- [20] M. Guzman, J. Dille, S. Godet, *Nanomed: Nanotechn. Biol. Med.*, **2012**, 8: 37–45.
- [21] C. Krishnaraj, E.G. Jagan, S. Rajasekar, P. Selvakumar, P.T. Kalaichelvan, N. Mohan, *Colloids Surf. Biointerfaces.*, **2012**, 76: 50–56.
- [22] S.K. Sivaraman, I. Elango, S. Kumar, V. Santhanam, *Curr. Sci.*, **2009**, 97, 7, 155–159.
- [23] M. Darroudi, M.B. Ahmad, A.H. Abdullah, N.A. Ibrahim, K. Shameli, *Int. J. Mol. Sci.*, **2010**, 11, 3898–3905.
- [24] A.S. Lanje, S.J. Sharma, R.B. Pode, *J. Chem. Pharm. Res.*, **2010**, 2, 478–483.
- [25] S. Burt, *Int. J. Food Microbiol.*, **2004**, 94: 223–253.
- [26] K.B. Narayanan, N. Sakthivel, *Mater. Res. Bull.*, **2011**, 46, 1708–1713.
- [27] P.U. Rani, P. Rajasekharreddy, *Colloid Surf., A* **2011**, 389, 188–194.
- [28] R. Vila, *Flavonoids and further Polyphenols in the genus Thymus*, Thyme, Tyler and Francis, London, 2002.
- [29] S. Burt, *Int. J. Food Microbiol.* **2004**, 94, 223–253.
- [30] K. Ashish, K. Ramit, S. Samita, S. Vikas, J. Bhaibhav, *J. Pharm. Res.*, **2012**, 1(3), 277.
- [31] P.D. Bragg, D.J. Rainnie, *Can. J. Microbiol.*, **1974**, 20, 883–889.
- [32] N. Ahmad, S. Sharma, V.N. Singh, S.F. Shamsi, A. Fatma, B.R. Mehta, *Biotech. Res. Int.*, **2011**, 8, 1–8.
- [33] A.D. Russell, W.B. Hugo, *Prog. Med. Chem.*, **1994**, 31, 351–370.
- [34] R.R. Larkin, D.R. Fravel, *Plant Diseases.*, **1998**, 82, 1022–1028.
- [35] G.N. Agrios, *Plant Pathology*, 3rd. ed. Academic Press, Inc.: New York. **1988**, 803pp.
- [36] E.I. Rabea, W. Steurbaut, *Plant Protect. Sci.*, **2010**, 46, 149–158.
- [37] F. Gao, C. Dai, X. Liu, *Afr. J. Microbiol. Res.*, **2010**, 4, 1346–1351.